Water Reuse

© 2023 The Authors

Water Reuse Vol 13 No 2, 193 doi: 10.2166/wrd.2023.081

Fenton process enhanced by metal sulfide for treating the actual evaporated mother liquid of gas field wastewater

Bing Yao, Ying Chen, Mengzhe Wang and Min Liu*

College of Architecture and Environment, Sichuan University, Chengdu 610065, China
*Corresponding author. E-mail: liuminscu@163.com

ABSTRACT

Evaporated mother liquor of gas field wastewater (EML-GFW) is a form of wastewater generated by the triple-effect evaporation treatment of gas field wastewater containing complex pollutants. In this study, four metal sulfides, CuS, ZnS, MoS_2, and WS_2, were used to strengthen the Fenton process in EML-GFW treatment. The optimum Fenton/ZnS process for the highest removal of TOC from EML-GFW was achieved at the initial pH of 3.0 and in a mixture of $FeSO_4{\cdot}7H_2O$:ZnS:H_2O_2 in the ratio of 30 g/L:10 g/L:1.2 mol/L, with a TOC removal efficiency of 74.5%. The organic components analysis of EML-GFW over four distinct periods demonstrated that the presence of *N*,*N*-dimethylethanolamine (DMEA) persisted and accounted for the greatest proportion of pollutants, identifying it as the characteristic pollutant. The TOC removal mechanism by Fenton/ZnS was revealed via analysis of organic materials obtained from the Fenton/ZnS process, tert-butanol quenching experiment, and illumination experiment. ZnS-generated hole–electron pairs under illumination, which promoted the reduction of Fe^{3+} to Fe^{2+}, followed by an acceleration of •OH generation, thus improving TOC removal efficiency. The Fenton/ZnS process improved the treatment of EML-GFW in the laboratory, providing strong data support and theoretical guidance for expanding this technology at the gas field project site.

Key words: evaporated mother liquor, Fenton/ZnS, gas field wastewater, *N*, *N*-dimethylethanolamine, total organic carbon (TOC)

HIGHLIGHTS

- The optimization of the Fenton/ZnS process was based on the actual wastewater.
- The TOC removal efficiency of EML-GFW reached 74.5% by the optimum Fenton/ZnS process.
- ZnS accelerated the production of •OH, increasing the removal efficiency of TOC.
- This work was meaningful for the wastewater treatment at the gas field project site.

GRAPHICAL ABSTRACT

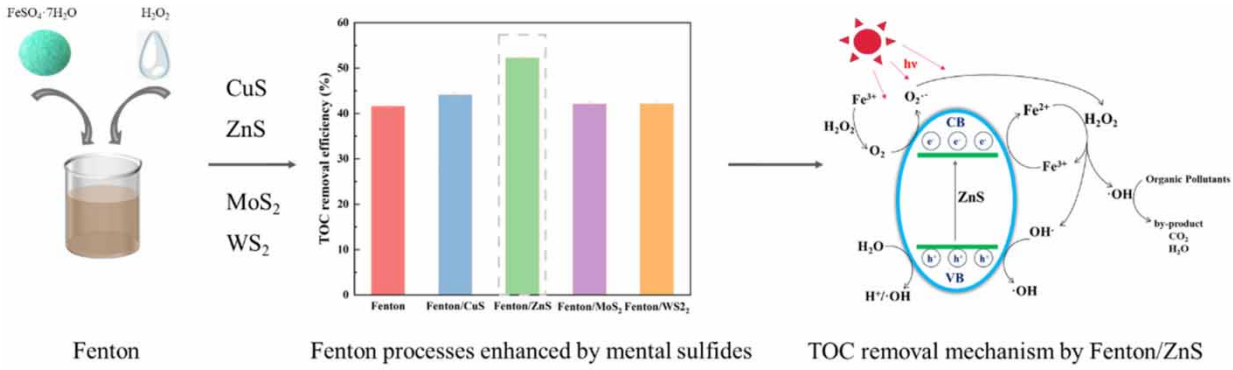

1. INTRODUCTION

Natural gas is considered low-carbon clean energy that ranks between traditional fossil fuels, such as oil and coal, and renewable energy. Natural gas emits less carbon than coal and oil and is cheaper than renewable energy, making it a suitable platform to foster China's energy transition toward achieving effective air pollution control and carbon neutrality (Ibrahim

et al. 2022). China's natural gas production has increased recently, reaching 1,925.0 billion m^3 at the end of 2020 (Resources 2021). However, during natural gas extraction, a huge volume of gas field wastewater is generated, including drilling wastewater, fracturing flow-back fluid, and high-salt wastewater (Feng *et al.* 2020; Jin *et al.* 2022). In addition, the triple-effect evaporation process has been identified as an effective technique for treating gas field wastewater due to the operability of evaporation equipment at the site of the gas field project. However, the evaporated mother liquor of gas field wastewater (EML-GFW), the concentrated liquid remaining after distillation, contains a range of organic compounds and inorganic salt ions at significantly higher concentrations than raw water (Wang *et al.* 2019; Feng *et al.* 2022).

There are only a handful of studies conducted on the actual EML-GFW due to the complexity of actual wastewater. EML-GFW removal using traditional adsorption methods, air flotation separation, and coagulation could only transform the phases of pollutants, thus necessitating additional treatment. In addition, a high-salt concentration leads to membrane fouling, thermal equipment scaling, and microbial death, thus hindering the application of these methods in EML-GFW treatment (Moussa *et al.* 2006; Osaka *et al.* 2008; Sheng *et al.* 2022).

The Fenton method is an established advanced oxidation technique (AOP) used to degrade refractory organic pollutants due to its strong oxidizing ability, fast reaction speed, and high treatment efficiency (Adil *et al.* 2020; Wang *et al.* 2021; Ziembowicz & Kida 2022). However, the decomposition efficiency of H_2O_2 in conventional Fenton is limited because of the weak cyclic reaction of Fe^{2+}/Fe^{3+}, which requires a catalyst or activator to accelerate Fe^{2+} regeneration (Liu *et al.* 2018; Ren *et al.* 2022). Metal sulfides are abundant in nature and have good electrical conductivity and strong stability, making them an ideal catalyst candidate to accelerate the speed and efficiency of pollutant removal by AOP (Fu & Lee 2019; Zhu *et al.* 2020; Li *et al.* 2021; Kumar *et al.* 2022). A diversity of metal sulfides have been reported to act as excellent catalysts to enhance •OH production, including CuS, MoS_2, WS_2, ZnS, Cr_2S_3, CoS_2, PbS, and so on. Xing *et al.* used the Fenton methods enhanced by various metal sulfides (MoS_2, WS_2, ZnS, Cr_2S_3, CoS_2, and PbS) to treat 20 mg/L rhodamine B (RhB). The results revealed that not only had the removal efficiency of RhB reached more than 90%, but also the reaction rate constant of RhB removal by the Fenton/MoS_2 method (3.7×10^{-2}/s) was 18.5 times higher than that of the conventional Fenton method (0.2×10^{-2}/s) (Xing *et al.* 2018). Dong *et al.* reported that in the WS_2 co-catalytic photoassisted Fe(II)/H_2O_2 Fenton system, accompanied by improved H_2O_2 decomposition efficiency, it was able to oxidize phenol (10 mg/L) and reduce Cr(VI) (40 mg/L) simultaneously, with removal efficiencies of 80.9 and 90.9%, respectively (Dong *et al.* 2018).

Four metal sulfides (CuS, ZnS, MoS_2, and WS_2) were used to enhance the Fenton process and to determine the process with the highest efficiency for actual EML-GFW. Based on the fundamental factors, namely the reaction time, initial pH of the solution, and the dosage of H_2O_2 and metal sulfides, optimization of the metal sulfide-enhanced process was conducted. Finally, simulated wastewater of characteristic pollutants, *N*,*N*-dimethylethanolamine (DMEA), was prepared to explore the TOC removal mechanism by Fenton/ZnS without the interference of complex organic matters in actual EML-GFW. This research offers theoretical insight into the implementation of the Fenton process, particularly for treating organic wastewater with complex constituents.

2. MATERIALS AND METHODS

2.1. Materials

EML-GFW was collected from a gas production plant in the Northeast Sichuan Province, China, where the gas field wastewater was first subjected to a pre-treatment process, followed by a treatment using the triple-effect evaporation technology to obtain EML-GFW. In addition to its poor biodegradability (B/C = 0.20), EML-GFW was found to contain salts in a high concentration. In Figure 1, the organic components analysis of EML-GFW differs substantially between the first batch (stored for 2 years), second batch, and third batch of EML-GFW, except for one common finding: the presence of DMEA as one of the major constituents in all batches. While the organic matters in EML-GFW typically react and transform with one another, the primary pollutant, DMEA, proved difficult to convert. Therefore, DMEA was identified as a characteristic organic pollutant of EML-GFW. Considering the complexity of actual EML-GFW, DMEA-simulated wastewater (DSW) was created to explore the removal mechanism of organic pollutants. In addition, all actual EML-GFW was obtained from the freshest third batch for all experiments conducted, and water quality is presented in Table 1.

Sulfuric acid (H_2SO_4), sodium hydroxide (NaOH), hydrogen peroxide (H_2O_2, 30%, w/w), ferrous sulfate heptahydrate ($FeSO_4{\cdot}7H_2O$), tert-butanol ($(CH_3)_3COH$), copper sulfide (CuS), molybdenum disulfide (MoS_2), zinc sulfide (ZnS), tungsten

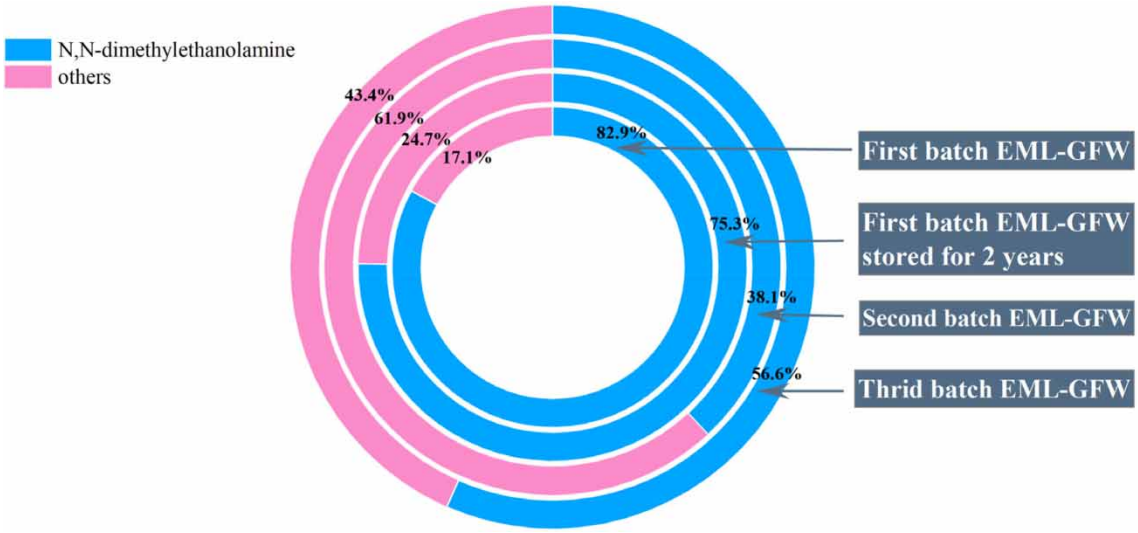

Figure 1 | The organic matter compositions of the first batch, first batch (stored for 2 years), second batch, and third batch EML-GFW wastewater by GC-MS spectra.

Table 1 | Indicators for water quality of EML-GFW for all the experiments conducted

Characteristics	Unit	Value
pH	–	13.5
Chemical oxygen demand (COD)	mg/L	1.12×10^4
Biochemical oxygen demand (BOD_5)	mg/L	2.21×10^3
Ammonia nitrogen (N)	mg/L	1.12
Suspended solids (SS)	mg/L	2.14×10^2
Petroleum	mg/L	5.80×10^{-1}
Volatile phenols (Phenol)	mg/L	9.00×10^{-2}
Total alkalinity ($CaCO_3$)	mg/L	4.92×10^4
Chloride	mg/L	8.50×10^4
Sulfate	mg/L	1.44×10^4
Conductivity	μS/cm	1.60×10^3
TOC	mg/L	1.55×10^3

disulfide (WS_2), dimethylamine ($(CH_3)_2NH$), *N*,*N*-dimethylethanolamine ($(CH_3)_2NCH_2CH_2OH$) used were all of the analytically pure (AR) grade. Distilled water was used in the experiments.

2.2. Experimental procedures

2.2.1. Batch experiments on the TOC removal effect of EML-GFW

The pH of 100 mL of EML-GFW was adjusted to 4.0 with sulfuric acid and subsequently added with 22 g/L $FeSO_4{\cdot}7H_2O$ and 20 g/L metal sulfides (CuS, ZnS, MoS_2, or WS_2) with vigorous stirring. After a reaction with 0.8 mol/L H_2O_2 for 3 h, the Fenton reaction was terminated. The supernatant of the precipitated solution was passed through a filter with a pore of 0.45 μm in diameter to measure TOC, followed by the screening of metal sulfides with the best treatment efficiency. Then, the effects of reaction time (1, 2, 3, 4, 5, and 6 h), initial pH of the solution (2.0, 3.0, 4.0, 5.0, 6.0, and 7.0), the dosage of H_2O_2 (0.2, 0.4, 0.6, 0.8, 1.0, 1.2, and 1.4 mol/L), $FeSO_4{\cdot}7H_2O$ (10, 15, 20, 25, 30, 35, and 40 g/L) and metal sulfide (0, 2, 4, 6, 8, 10, and 12 g/L) on EML-GFW were investigated. All experiments were performed three times to ensure the accuracy and reliability of the results.

2.2.2. Identification of active substances in DSW treatment

Based on DMEA concentration in the actual wastewater (EML-GFW), the simulated wastewater (DSW) was prepared with 386 mg/L DMEA. Fenton/ZnS process dosages were adjusted in proportions equal to the TOC ratios of EML-GFW and DSW.

The pH of DSW was adjusted to 3.0, and 1 mol/L tert-butanol was added. After fully dissolving 4.6 g/L $FeSO_4{\cdot}7H_2O$ and 1.5 g/L metal sulfide in DSW, 0.185 mol/L H_2O_2 was slowly added. Following the termination of the Fenton reaction, the supernatant was passed through a filter membrane with a pore size of 0.45 μm and subjected to DMEA concentration determination.

2.2.3. Effect of light on DSW treatment

The foil wrap was used to block the light and the next steps were performed according to Section 2.2.2. All experiments were conducted three times to ensure the accuracy and reliability of the results.

2.3. Analytical methods

TOC measurement (vario TOC select, Germany) was conducted according to the combustion oxidation-non-dispersive infrared absorption method. pH was measured by a microelectrode system (unisense mmm 7221, Danish).

EML-GFW samples were subjected to solid-phase micro-extraction and analyzed by gas chromatography-mass spectrometry (GC-MS) to qualitatively determine the compositions of organic compounds. GC-MS analysis was carried out using the following protocols: DB-624UI (60 m × 0.25 mm × 1.40 μm) column; temperature procedures: 40 °C for 5 min, followed by a gradual increment to 150 °C at a rate of 5 °C/min, the final increment to 280 °C at a rate of 10 °C/min, and a holding time of 7 min; high-purity helium as a carrier gas; a diversion ratio of 3.0. The full scan mode was adopted at the scan range of 33–500 amu. Finally, the retention time of the compound was compared with the NIST database to determine the quality of the results. These tests were completed at the Analytical Testing Center of Sichuan University.

DMEA concentration was determined by gas chromatography using the following parameters: CAM (30 m × 0.32 mm × 0.25 μm) column; temperature procedure: 60 °C for 5 min, followed by the increment to 200 °C at a rate of 20 °C/min, and a holding time of 4 min. The injection volume was 1 μL and nitrogen was used as the carrier gas at a flow rate of 25 cm/s.

3. RESULTS AND DISCUSSION

3.1. TOC removal effect of EML-GFW by the enhanced Fenton process

To determine the capacity of metal sulfides in enhancing the Fenton process, five experiments were conducted by adding CuS, ZnS, MoS_2, or WS_2 into an EML-GFW solution as described in Figure 2. The TOC removal efficiencies of the Fenton process enhanced with the addition of CuS, ZnS, MoS_2, or WS_2 were 41.6, 44.1, 52.3, and 42.1%, respectively. The results depict that the highest enhancement of efficiency of the Fenton process was achieved by adding ZnS, possibly attributed to the photocatalytic activity of ZnS. Unlike the classical Fenton process, the presence of a semiconductor material, ZnS, was capable of acting as a catalyst by absorbing the visible light with energy greater than or equal to its band gap, causing the excitation of valence band electrons in the conduction band. The electrons and holes induced by light could further generate •OH as displayed in Equations (9)–(13, followed by redox contaminants, consistent with the results of Xing *et al.* (Wang *et al.* 2008; Lee & Wu 2017; Xing *et al.* 2018; Manny Porto Barros *et al.* 2023). In addition, the Fe^{3+} generated during the Fenton process could accept the electrons generated from the visible light irradiation of ZnS. Enhancing the Fe^{3+}/Fe^{2+} cycle can effectively ensure H_2O_2 decomposition and thus, the continuous generation of free radicals, avoiding the blockage after complete depletion of Fe^{2+}. Simultaneously, it effectively reduced the compounding of photogenerated electrons with holes (Guo *et al.* 2022; Zhang & Chu 2022). The photocatalytic activities of CuS, MoS_2, and WS_2 were weaker than those of ZnS, resulting in less effective treatment.

3.2. Optimization of the Fenton/ZnS process

The optimization of the Fenton/ZnS process was conducted based on several factors: reaction time, initial solution pH, as well as the dosages of H_2O_2, $FeSO_4{\cdot}7H_2O$, and ZnS.

3.2.1. Reaction time

Figure 3(a) displays the effect of reaction time within 6 h on the TOC removal by ZnS-enhanced Fenton. In the first 3 h, TOC removal efficiency increased slightly and finally reached 52.8%. After 6 h of reaction, TOC removal efficiency slightly increased

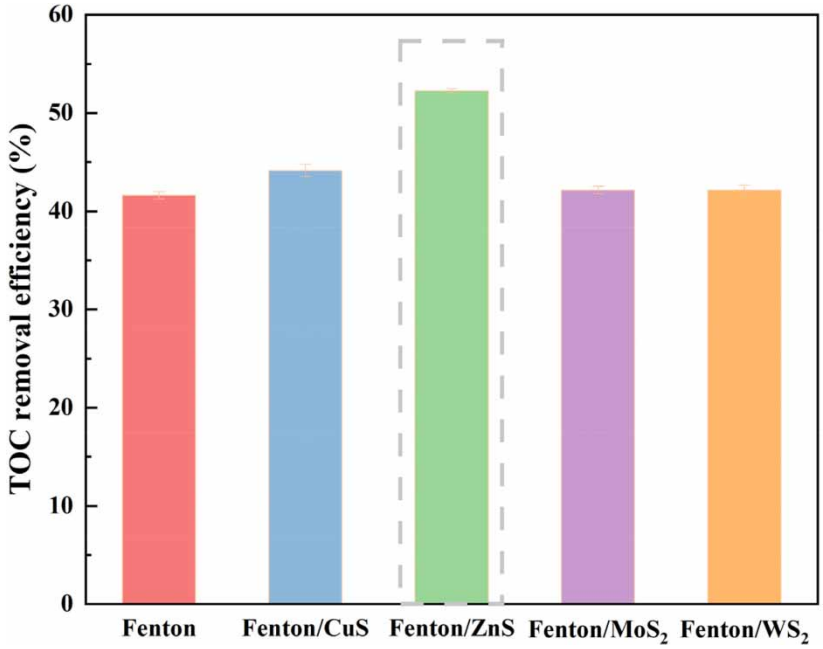

Figure 2 | Effect of different metal sulfides on TOC removal efficiency of EML-GFW. (The initial pH was 4.0; the concentration of $FeSO_4{\cdot}7H_2O$, metal sulfides, and H_2O_2 was 22, 20, and 0.8 mol/L, respectively; the reaction time was 3 h).

to 53.5%, without significant improvement. At the initial stage of the reaction, Fe^{2+} reacted with H_2O_2 to generate •OH as described by Equation (1), which could effectively mineralize pollutants, and Fe^{3+} produced during this period was reduced to Fe^{2+} according to Equations (2) and (3) due to ZnS photocatalysis, resulting in a decreased TOC concentration (Chen *et al.* 2019; Guo *et al.* 2021). However, in addition to the low rate constant of the reaction as illustrated in Equation (2), the active sites of ZnS in EML-GFW might be masked by impurities, causing Fe^{3+} to accumulate in significant amounts while the catalyst, Fe^{2+}, continued to decrease as the reaction progressed, lowering the rate of mineralization. Extending the reaction time could not improve TOC removal; consequently, 3 h is the optimum reaction time for the enhanced Fenton process.

$$Fe^{2+} + H_2O_2 \rightarrow Fe^{3+} + OH^- + \bullet OH \quad (1)$$

$$Fe^{3+} + H_2O_2 \rightarrow Fe^{2+} + HO_2\bullet + H^+ \quad (2)$$

$$Fe^{3+} + HO_2\bullet \rightarrow Fe^{2+} + O_2 + H^+ \quad (3)$$

3.2.2. Initial pH of the solution

Generally, the oxidation in the Fenton process was found to be highest under acidic conditions; accordingly, the Fenton/ZnS process for treating EML-GFW was conducted using initial pH values of 2.0, 3.0, 4.0, 5.0, 6.0, and 7.0 for 3 h (Figure 3(b)). When pH increased from 2.0 to 3.0, TOC efficiency increased from 48.4 to 55.2%; however, a further increase to 7.0 significantly decreased the removal efficiency to 37.3%. Due to the better stability of solid ZnS at pH 3.0–11, the initial pH affected pollutant removal mainly by influencing the Fe^{2+}-catalyzed Fenton reaction, so the removal efficiency was higher under acidic than neutral conditions (Wang *et al.* 2011; Manny Porto Barros *et al.* 2023). H^+ in the solution exhibited a strong scavenging effect on •OH according to Equation (4) at pH 2.0 and a low TOC removal effect at pH 3.0. As pH continued to increase, Fe^{3+} in the solution was hydrolyzed and precipitated, which affected the catalytic ability of the catalyst, resulting in a significant decline in the treatment efficiency (Huang & Huang 2008; Navalon *et al.* 2011). The optimal initial reaction pH for the Fenton/ZnS process was 3.0.

$$\bullet OH + H^+ + e^- \rightarrow H_2O \quad (4)$$

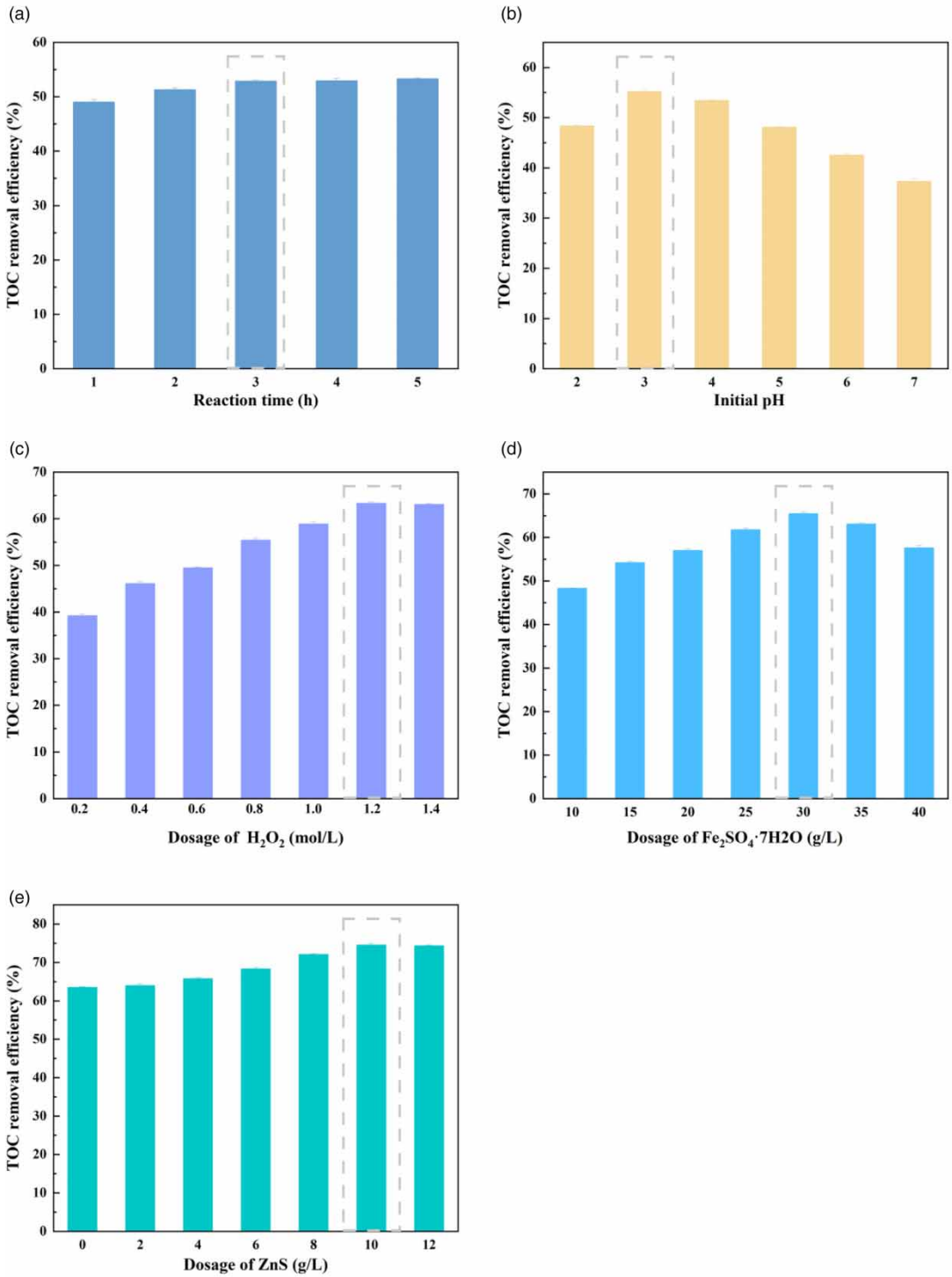

Figure 3 | Effect of reaction time (a); initial pH of the solution (b); dosage of H_2O_2 (c); $FeSO_4{\cdot}7H_2O$ (d); and ZnS (e) on TOC removal of EML-GFW.

3.2.3. H_2O_2 dosage

H_2O_2 is the main contributor of hydroxyl free radicals and the effect of its dosage on TOC removal via the Fenton/ZnS process at pH 3.0 after 3 h of reaction is demonstrated in Figure 3(c). When H_2O_2 dosage was increased from 0.2 to 1.2 mol/L, the removal efficiency of TOC increased from 39.2 to 63.3% as more •OH was produced to mineralize the organic matter.

However, when H_2O_2 dosage was further increased to 1.4 mol/L, the quenching effect on •OH would change to a state as described in Equation (5), which results in ineffective decomposition and is not conducive to the mineralization of organic compounds by •OH (Ramirez *et al.* 2007; Xue *et al.* 2009a, 2009b; Jiang *et al.* 2010). Adding excessive H_2O_2 would not only render the process expensive but also ineffective in improving the removal efficiency of TOC. Consequently, it was decided that 1.2 mol/L H_2O_2 is sufficient for optimum TOC removal via the Fenton/ZnS process.

$$H_2O_2 + \bullet OH \rightarrow H_2O + HO_2\bullet \quad (5)$$

3.2.4. $FeSO_4{\cdot}7H_2O$ dosage

Using Fe^{2+} as a catalyst could promote •OH production by H_2O_2, and thus the effect of different dosages of $FeSO_4{\cdot}7H_2O$ on the efficiency of the Fenton/ZnS process in treating EML-GFW was investigated as described in Figure 3(d). When $FeSO_4{\cdot}7H_2O$ was increased from 10 to 30 g/L, TOC removal efficiency increased from 48.3 to 65.5%; however, a further increase to 40 g/L resulted in a decreased value to 57.6%. Using $FeSO_4{\cdot}7H_2O$ at concentrations higher than 30 g/L reduced the TOC removal efficiency. In addition to promoting •OH quenching by Fe^{2+} as shown in Equation (6), the excessive ferric produces several mutually quenched •OH, as displayed in Equation (7), resulting in the loss of available •OH reducing organic mineralization efficiency (Liu *et al.* 2015). Furthermore, excess $FeSO_4{\cdot}7H_2O$ increases the amount of dye added for subsequent pH recovery, thus increasing the cost of wastewater treatment. Therefore, the optimal dosage of $FeSO_4{\cdot}7H_2O$ for the Fenton/ZnS process was determined to be 30 g/L.

$$Fe^{2+} + \bullet OH \rightarrow Fe^{3+} + OH^- \quad (6)$$

$$\bullet OH + \bullet OH \rightarrow H_2O_2 \quad (7)$$

3.2.5. ZnS dosage

ZnS addition was beneficial to improve the treatment effect of the Fenton/ZnS process on EML-GFW and the influence of its dosage on wastewater treatment is demonstrated in Figure 3(e). With the increase of ZnS dosage, TOC removal efficiency exhibited a trend of increasing, followed by stabilizing. The maximum TOC removal efficiency was 74.5% when ZnS dosage was increased from 0 to 12 g/L. The photocatalytic activity of ZnS helped improve the oxidation activity of Fenton because ZnS contributed to Fe^{3+} reduction to Fe^{2+} when illuminated, and the regenerated Fe^{2+} continued to react with H_2O_2 to generate more •OH, thus promoting the continuous progress of the Fenton reaction and the mineralization of organic pollutants (Xing *et al.* 2018). However, when ZnS was added in excess, TOC removal effect was not improved due to the limited oxidant H_2O_2 content in the solution. Meanwhile, the excess ZnS led to turbidity, which hindered photogenerated radiation and subsequently decreased catalyst efficiency. In addition, the formation of particle agglomerates impaired the excitation process and the formation of electron/hole pairs due to ZnS overdosing (Suave *et al.* 2018; Garg *et al.* 2019; Manny Porto Barros *et al.* 2023). Compared with the single Fenton method, the Fenton/ZnS process with 10 g/L ZnS addition could improve the TOC removal efficiency of EML-GFW by 32.9%.

Under optimized conditions, i.e., initial pH of 3.0, 30 g/L of $FeSO_4$ $7H_2O$, 10 g/L ZnS, and 1.2 mol/L H_2O_2, despite the presence of high salt and multiple organics in EML-GFW, TOC removal efficiency by the Fenton/ZnS process could reach up to 74.5% after 3 h of reaction.

3.3. Mechanism of DSW treatment by the Fenton/ZnS process

3.3.1. Analysis of organics after the Fenton/ZnS process

DMEA was undetected in EML-GFW and DSW subjected to the optimized Fenton/ZnS process and TOC removal efficiencies were recorded as 74.5 and 46.1%, respectively, indicating the easy removal yet difficult mineralization of DMEA. The main organic compounds identified in DSW subjected to the Fenton/ZnS process include dimethylamine, with a relative percentage of 90.8%, suggesting that part of DMEA might have completely mineralized to produce CO_2 and H_2O, and the rest was mainly oxidized to form dimethylamine, which remained in the solution.

3.3.2. Identification of active substances in DSW treatment by the Fenton/ZnS process

The potential rapid reaction between tert-butanol (TBA) and •OH at a rate of 6.0×10^8 L/(mol·s) is described by Equation (8), which is a quencher commonly used to demonstrate the presence of •OH (Witte *et al.* 2009; Lai *et al.* 2021). Based on Figure 4,

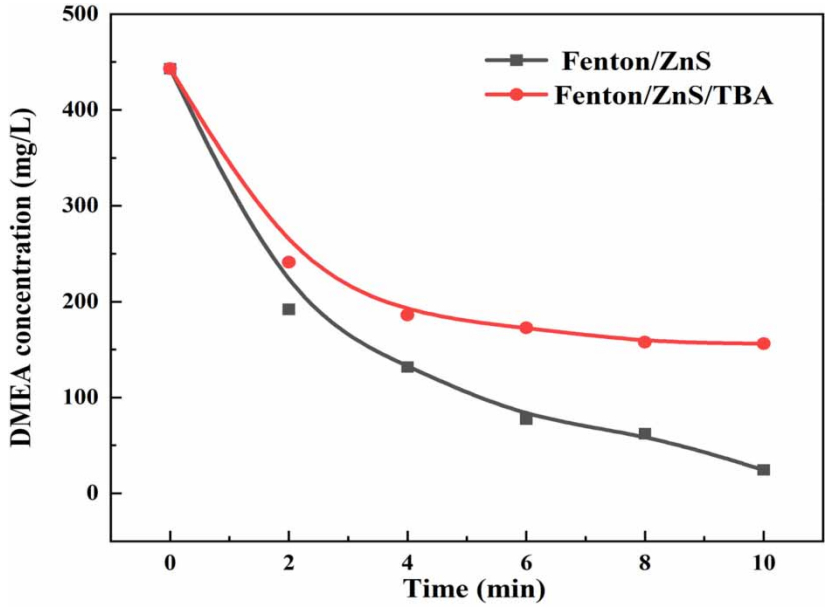

Figure 4 | Effect of TBA on DSW treatment via the optimized Fenton/ZnS process. (The initial pH was 3.0; the dosages of $FeSO_4{\cdot}7H_2O$, H_2O_2, ZnS, and tert-butanol were 4.6 g/L, 0.185 mol/L, 1.5 g/L, and 1 mol/L, respectively; the reaction time was 10 min).

DMEA concentration decreased from 94.5 to 64.8% with TBA addition at 10 min, indicating a significant inhibition of DMEA removal by TBA in the Fenton/ZnS process, with •OH playing an important role in DSW mineralization.

$$(CH_3)_3COH + \bullet OH \rightarrow H_2O + \bullet CH_2(CH_3)_2COH \quad (8)$$

3.3.3. Effect of light on DSW treatment by the Fenton/ZnS process

ZnS is a semiconductor material often used in the photocatalytic treatment of wastewater (Zhang *et al.* 2011; Hao *et al.* 2018). Under shading and illumination, DSW treatment by the Fenton/ZnS is shown in Figure 5. TOC removal efficiency via the Fenton/ZnS process without shading was 46.1%, while under shading conditions, the efficiency was 27.3%, indicating the role of light in creating a conducive environment to DMEA mineralization via the Fenton/ZnS process. The possible mechanism of EML-GFW treatment via the Fenton/ZnS process is depicted in Figure 6. ZnS-generated electrons and holes under illumination as in Equation (9), both favoring the induction of free radicals. The photogenerated electrons reduced Fe^{3+} in the solution to Fe^{2+}, thereby promoting •OH generation in the Fenton reaction. Simultaneously, photogenerated electrons reacted with O_2 to produce $\bullet O_2^-$ as expressed by Equation (10), generating H_2O_2 as expressed by Equation (11), which further supported the continuous progress of the Fenton reaction. In addition, photogenic holes might react with H_2O or OH^- to produce •OH as described in Equations (12) and (13) (Rajeshwar *et al.* 2008; Zhu *et al.* 2019). •OH generated in these processes could oxidize DMEA to form by-products, dimethylamine, or even mineralizing to CO_2 and H_2O.

$$ZnS + h\nu \rightarrow ZnS(e^-) + ZnS(h^+) \quad (9)$$

$$ZnS(e^-) + O_2 \rightarrow \bullet O_2^- \quad (10)$$

$$\bullet O_2^- + ZnS(e^-) + 2H^+ \rightarrow H_2O_2 \quad (11)$$

$$ZnS(h^+) + H_2O \rightarrow H^+ + \bullet OH \quad (12)$$

$$ZnS(h^+) + OH^- \rightarrow \bullet OH \quad (13)$$

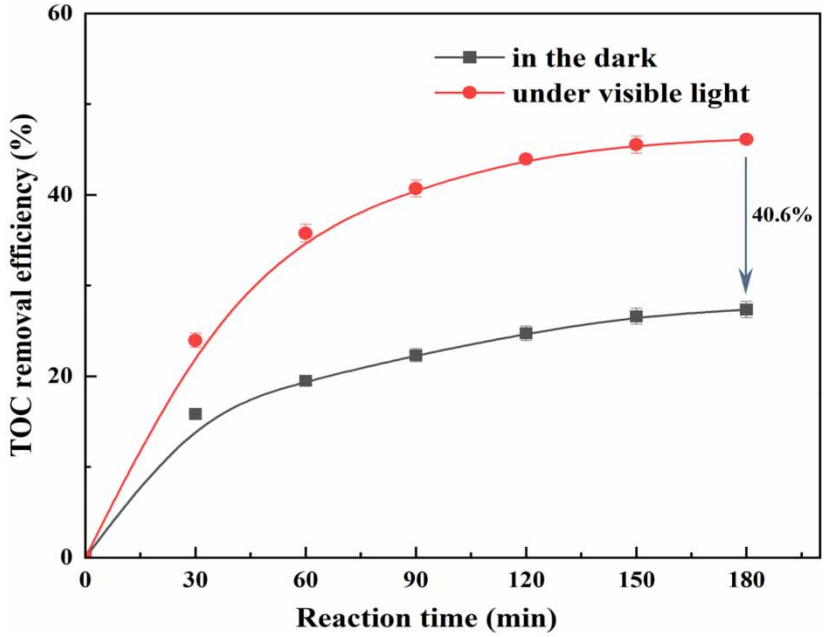

Figure 5 | Effect of light condition on DSW treatment via the optimized Fenton/ZnS process. (The initial pH was 3.0; the dosages of $FeSO_4{\cdot}7H_2O$, H_2O_2, and ZnS were 4.6 g/L, 0.185 mol/L, and 1.5 g/L, respectively; the reaction time was 3 h).

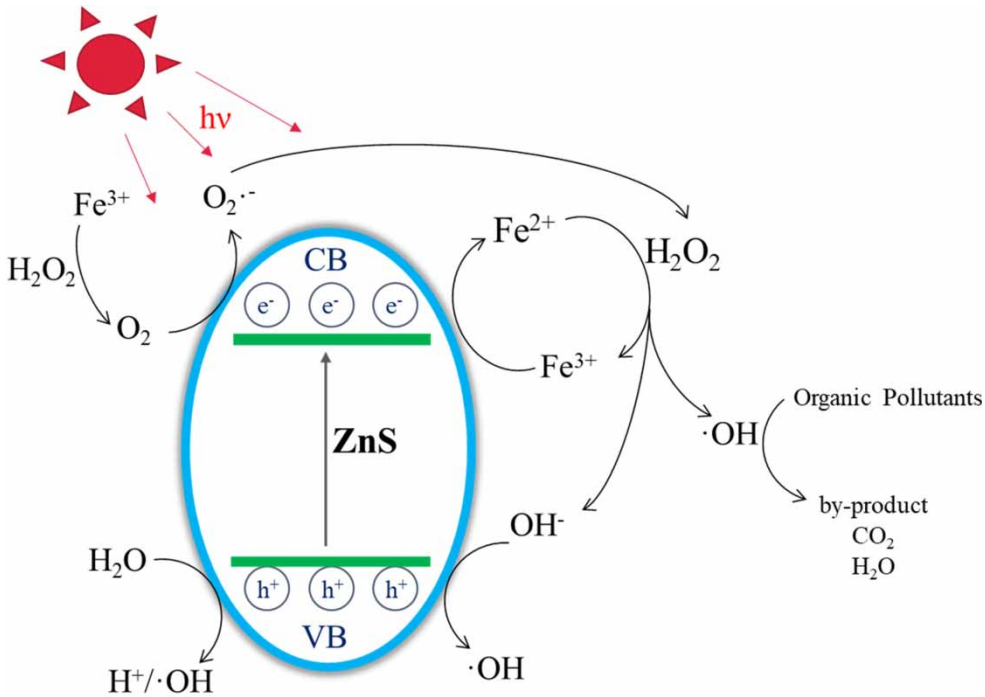

Figure 6 | Mechanism of EML-GFW treatment via the optimized Fenton/ZnS process. (The initial pH was 3.0; the dosages of $FeSO_4{\cdot}7H_2O$, H_2O_2, and ZnS were 4.6 g/L, 0.185 mol/L, and 1.5 g/L, respectively; the reaction time was 3 h).

4. CONCLUSION

The effects of the Fenton process enhanced by metal sulfides (CuS, ZnS, MoS_2, and WS_2) on actual EML-GFW were investigated, revealing that the optimum condition was achieved by applying the Fenton/ZnS process. The TOC removal efficiency

of EML-GFW reached 74.5% when the process was carried out with an initial pH of 3.0, and the doses of $FeSO_4{\cdot}7H_2O$, ZnS, and H_2O_2 used were 30, 10 g/L, and 1.2 mol/L, respectively. Furthermore, GC-MS analysis identified DMEA as one of the main pollutants of EML-GFW at different time points. Finally, the mechanism of DSW treatment via the Fenton/ZnS process was proposed. The photocatalytic activity of ZnS under illumination could accelerate the Fenton reaction by promoting the production of the active component, •OH, increasing the removal efficiency of TOC. In summary, the Fenton/ZnS process may allow for a better treatment efficiency of the actual wastewater EML-GFW composed of complex organic contaminants in the laboratory, offering valuable insights for application in wastewater treatment at the gas field project site.

AUTHOR CONTRIBUTIONS

B.Y. conceptualized the system, investigated the study, did a formal analysis, and wrote the original draft. Y.C. and M.L. supervised the study, wrote the review, edited the file, managed resources, and acquired funds. M.W. investigated the study, wrote the review and edited the file.

FUNDING

This study was supported by the National Major Science and Technology Project of the 13th Five-Year Plan 'High-efficiency development of ultra-deep bio-herm gas reservoirs with bottom water' of China (2016ZX05017-005).

DATA AVAILABILITY STATEMENT

All relevant data are included in the paper or its Supplementary Information.

CONFLICT OF INTEREST

The authors declare there is no conflict.

REFERENCES

Adil, S., Maryam, B., Kim, E.-J. & Dulova, N. 2020 Individual and simultaneous degradation of sulfamethoxazole and trimethoprim by ozone, ozone/hydrogen peroxide and ozone/persulfate processes: a comparative study. *Environmental Research* **189**, 109889.

Chen, M., Zhang, Z., Zhu, L., Wang, N. & Tang, H. 2019 Bisulfite-induced drastic enhancement of bisphenol A degradation in Fe^{3+}-H_2O_2 Fenton system. *Chemical Engineering Journal* **361**, 1190–1197.

Dong, C., Ji, J., Shen, B., Xing, M. & Zhang, J. 2018 Enhancement of H2O2 Decomposition by the Co-catalytic Effect of WS2 on the Fenton Reaction for the Synchronous Reduction of Cr(VI) and Remediation of Phenol. *Environmental Science & Technology* **52**, 11297–11308.

Feng, H., Liu, M., Zeng, W. & Chen, Y. 2020 Optimization of the O_3/H_2O_2 process with response surface methodology for pretreatment of mother liquor of gas field wastewater. *Frontiers of Environmental Science & Engineering* **15**, 78.

Feng, H., Liu, M., Zeng, W., Chen, Y., Wang, M., Yuan, L. & Yu, Z. 2022 Feasibility of resource utilization of the refractory evaporation concentrate of gas field wastewater exhibiting high salinity: Application of UV/Fenton, desulfurization, distillation and crystallization process after pre-treatment. *Environmental Research* **204**, 112317.

Fu, G. & Lee, J.-M. 2019 Ternary metal sulfides for electrocatalytic energy conversion. *Journal of Materials Chemistry A* **7** (16), 386–9405.

Garg, A., Singhania, T., Singh, A., Sharma, S., Rani, S., Neogy, A., Yadav, S. R., Sangal, V. K. & Garg, N. 2019 Photocatalytic degradation of bisphenol-A using N, Co codoped TiO_2 catalyst under solar light. *Scientific Reports* **9** (1), 765.

Guo, J., Zhou, Y., Yu, M., Liang, H. & Niu, J. 2021 The roles of wavelength in the gaseous toluene removal with OH from UV activated Fenton reagent. *Chemosphere* **275**, 129998.

Guo, W., Li, T., Chen, Q., Wan, J., Zhang, J., Wu, B. & Wang, Y. 2022 Construction of Fe^{2+}/Fe^{3+} cycle system at dual-defective carbon nitride interfaces for photogenerated electron utilization. *Separation and Purification Technology* **285**, 120357.

Hao, X., Zhou, J., Cui, Z., Wang, Y., Wang, Y. & Zou, Z. 2018 Zn-vacancy mediated electron-hole separation in ZnS/g-C_3N_4 heterojunction for efficient visible-light photocatalytic hydrogen production. *Applied Catalysis B: Environmental* **229**, 41–51.

Huang, C.-P. & Huang, Y.-H. 2008 Comparison of catalytic decomposition of hydrogen peroxide and catalytic degradation of phenol by immobilized iron oxides. *Applied Catalysis A: General* **346**, 140–148.

Ibrahim, M. F., Hod, R., Ahmad Tajudin, M. A. B., Wan Mahiyuddin, W. R., Mohammed Nawi, A. & Sahani, M. 2022 Children's exposure to air pollution in a natural gas industrial area and their risk of hospital admission for respiratory diseases. *Environmental Research* **210**, 112966.

Jiang, C., Pang, S., Ouyang, F., Ma, J. & Jiang, J. 2010 A new insight into Fenton and Fenton-like processes for water treatment. *Journal of Hazardous Materials* **174**, 813–817.

Jin, X., Zhang, L., Liu, M., Hu, S., Yao, Z., Liang, J., Wang, R., Xu, L., Shi, X., Bai, X., Jin, P. & Wang, X. C. 2022 Characteristics of dissolved ozone flotation for the enhanced treatment of bio-treated drilling wastewater from a gas field. *Chemosphere* **298**, 134290.

Kumar, N., Verma, S., Park, J., Chandra Srivastava, V. & Naushad, M. 2022 Evaluation of photocatalytic performances of PEG and PVP capped zinc sulfide nanoparticles towards organic environmental pollutant in presence of sunlight. *Chemosphere* **298**, 134281.

Lai, X., Ning, X.-a., Zhang, Y., Li, Y., Li, R., Chen, J. & Wu, S. 2021 Treatment of simulated textile sludge using the Fenton/Cl^- system: the roles of chlorine radicals and superoxide anions on PAHs removal. *Environmental Research* **197**, 110997.

Lee, G.-J. & Wu, J. J. 2017 Recent developments in ZnS photocatalysts from synthesis to photocatalytic applications – a review. *Powder Technology* **318**, 8–22.

Li, Y., Dong, H., Li, L., Tang, L., Tian, R., Li, R., Chen, J., Xie, Q., Jin, Z., Xiao, J., Xiao, S. & Zeng, G. 2021 Recent advances in waste water treatment through transition metal sulfides-based advanced oxidation processes. *Water Research* **192**, 116850.

Liu, W., Wang, Y., Ai, Z. & Zhang, L. 2015 Hydrothermal synthesis of FeS_2 as a high-efficiency Fenton reagent to degrade alachlor via superoxide-mediated Fe(II)/Fe(III) cycle. *ACS Applied Materials & Interfaces* **7**, 28534–28544.

Liu, J., Dong, C., Deng, Y., Ji, J., Bao, S., Chen, C., Shen, B., Zhang, J. & Xing, M. 2018 Molybdenum sulfide co-catalytic Fenton reaction for rapid and efficient inactivation of *Escherichia coli*. *Water Research* **145**, 312–320.

Manny Porto Barros, M., Costa Almeida, K. J., Vinicius Sousa Conceição, M., Henrique Pereira & D., Botelho, G. 2023 Photodegradation of bisphenol A by ZnS combined with H_2O_2: evaluation of photocatalytic activity, reaction parameters, and DFT calculations. *Journal of Molecular Liquids* **371**, 121096.

Moussa, M. S., Sumanasekera, D. U., Ibrahim, S. H., Lubberding, H. J., Hooijmans, C. M., Gijzen, H. J. & van Loosdrecht, M. C. M. 2006 Long term effects of salt on activity, population structure and floc characteristics in enriched bacterial cultures of nitrifiers. *Water Research* **40**, 1377–1388.

Navalon, S., Miguel, M. D., Martin, R., Alvaro, M. & Garcia, H. 2011 Enhancement of the catalytic activity of supported gold nanoparticles for the Fenton reaction by light. *Journal of the American Chemical Society* **133**, 2218.

Osaka, T., Shirotani, K., Yoshie, S. & Tsuneda, S. 2008 Effects of carbon source on denitrification efficiency and microbial community structure in a saline wastewater treatment process. *Water Research* **42**, 3709–3718.

Rajeshwar, K., Osugi, M. E., Chanmanee, W., Chenthamarakshan, C. R., Zanoni, M. V. B., Kajitvichyanukul, P. & Krishnan-Ayer, R. 2008 Heterogeneous photocatalytic treatment of organic dyes in air and aqueous media. *Journal of Photochemistry and Photobiology C: Photochemistry Reviews* **9**, 171–192.

Ramirez, J. H., Maldonado-Hódar, F. J., Pérez-Cadenas, A. F., Moreno-Castilla, C., Costa, C. A. & Madeira, L. M. 2007 Azo-dye Orange II degradation by heterogeneous Fenton-like reaction using carbon-Fe catalysts. *Applied Catalysis B: Environmental* **75**, 312–323.

Ren, Y., Zhang, J., Ji, C., Wang, S., Lv, L. & Zhang, W. 2022 Iron-based metal-organic framework derived pyrolytic materials for effective Fenton-like catalysis: performance, mechanisms and practicability. *Science of The Total Environment* **809**, 152201.

Resources, M. o. N. 2021 *China Mineral Resources 2021*.

Sheng, F., Li, X., Li, Y., Afsar, N. U., Zhao, Z., Ge, L. & Xu, T. 2022 Cationic covalent organic framework membranes for efficient dye/salt separation. *Journal of Membrane Science* **644**, 120118.

Suave, J., Jose, H. J. & Fatima, P. 2018 Photocatalytic degradation of polyvinylpyrrolidone in aqueous solution using TiO_2/H_2O_2/UV system. *Environmental Technology* **39**, 1404–1412.

Wang, X., Wan, F., Han, K., Chai, C. & Jiang, K. 2008 Large-scale synthesis well-dispersed ZnS microspheres and their photoluminescence, photocatalysis properties. *Materials Characterization* **59**, 1765–1770.

Wang, M., Zhang, Q., Hao, W. & Sun, Z.-X. 2011 Surface stoichiometry of zinc sulfide and its effect on the adsorption behaviors of xanthate. *Chemistry Central Journal* **5**, 73.

Wang, Y., Li, H.-q. & Ren, L.-M. 2019 Organic matter removal from mother liquor of gas field wastewater by electro-Fenton process with the addition of H_2O_2: effect of initial pH. *Royal Society Open Science* **6**, 191304.

Wang, C., Zhao, Z., Deng, X., Chen, R., Liang, J., Shi, W. & Cui, F. 2021 Ultrafast oxidation of emerging contaminants by novel VUV/Fe^{2+}/PS process at wide pH range: performance and mechanism. *Chemical Engineering Journal* **426**, 131921.

Witte, B. D., Langenhove, H. V., Hemelsoet, K., Demeestere, K., Wispelaere, P. D., Van Speybroeck, V. & Dewulf, J. 2009 Levofloxacin ozonation in water: rate determining process parameters and reaction pathway elucidation. *Chemosphere* **76**, 683–689.

Xing, M., Xu, W., Dong, C., Bai, Y., Zeng, J., Zhou, Y., Zhang, J. & Yin, Y. 2018 Metal sulfides as excellent co-catalysts for H_2O_2 decomposition in advanced oxidation processes. *Chem* **4**, 1359–1372.

Xue, X., Hanna, K., Abdelmoula, M. & Deng, N. 2009a Adsorption and oxidation of PCP on the surface of magnetite: kinetic experiments and spectroscopic investigations. *Applied Catalysis B: Environmental* **89**, 432–440.

Xue, X., Hanna, K. & Deng, N. 2009b Fenton-like oxidation of rhodamine B in the presence of two types of iron (II, III) oxide. *Journal of Hazardous Materials* **166**, 407–414.

Zhang, Y. & Chu, W. 2022 g-C_3N_4 induced acceleration of Fe^{3+}/Fe^{2+} cycles for enhancing metronidazole degradation in Fe^{3+}/peroxymonosulfate process under visible light. *Chemosphere* **293**, 133611.

Zhang, J., Yu, J., Zhang, Y., Li, Q. & Gong, J. R. 2011 Visible light photocatalytic H-2-production activity of CuS/ZnS porous nanosheets based on photoinduced interfacial charge transfer. *Nano Letters* **11**, 4774–4779.

Zhu, B., Cheng, H., Ma, J., Kong, Y. & Komarneni, S. 2019 Efficient degradation of rhodamine B by magnetically separable ZnS–$ZnFe_2O_4$ composite with the synergistic effect from persulfate. *Chemosphere* **237**, 124547.

Zhu, B., Cheng, H., Qin, Y., Ma, J., Kong, Y. & Komarneni, S. 2020 Copper sulfide as an excellent co-catalyst with $K_2S_2O_8$ for dye decomposition in advanced oxidation process. *Separation and Purification Technology* **233**, 116057.

Ziembowicz, S. & Kida, M. 2022 Limitations and future directions of application of the Fenton-like process in micropollutants degradation in water and wastewater treatment: a critical review. *Chemosphere* **296**, 134041.

First received 19 November 2022; accepted in revised form 7 February 2023. Available online 22 March 2023